Journal of Power Sources 196 (2011) 46–53

Contents lists available at ScienceDirect

Journal of Power Sources

journal homepage: www.elsevier.com/locate/jpowsour

Application of proton exchange membrane fuel cells for the monitoring and direct usage of biohydrogen produced by *Chlamydomonas reinhardtii*

S. Oncel*, F. Vardar-Sukan

Department of Bioengineering, Faculty of Engineering, Ege University, 35100 Bornova, Izmir, Turkey

ARTICLE INFO

Article history:
Received 13 December 2009
Received in revised form 10 June 2010
Accepted 17 July 2010
Available online 22 July 2010

Keywords:
Chlamydomonas reinhardtii
Proton exchange membrane
Fuel cells
Biohydrogen
Mass transfer
Mixing

ABSTRACT

Photo-biologically produced hydrogen by *Chlamydomonas reinhardtii* is integrated with a proton exchange (PEM) fuel cell for online electricity generation. To investigate the fuel cell efficiency, the effect of hydrogen production on the open circuit fuel cell voltage is monitored during 27 days of batch culture. Values of volumetric hydrogen production, monitored by the help of the calibrated water columns, are related with the open circuit voltage changes of the fuel cell. From the analysis of this relation a dead end configuration is selected to use the fuel cell in its best potential. After the open circuit experiments external loads are tested for their effects on the fuel cell voltage and current generation. According to the results two external loads are selected for the direct usage of the fuel cell incorporating with the photobioreactors (PBR). Experiments with the PEM fuel cell generate a current density of 1.81 mA cm^{-2} for about 50 h with 10 Ω load and 0.23 mA cm^{-2} for about 80 h with 100 Ω load.

1. Introduction

Increasing demands of energy, environmental concerns and depleting fossil resources have been pushing researchers all over the world to find novel solutions to this global challenge [1–4].

In a quest to overcome these problems many experts have been advocating the usage of hydrogen as the fuel of the future. One of the major goals is the production of renewable H_2 fuel on large scale using economically favorable raw materials and processes including renewable sources. Biophotolysis (direct and indirect) of water by using algae and cyanobacteria, photo-fermentation of organic compounds by photosynthetic bacteria, dark fermentation of organic compounds, or combination of these processes (hybrid systems using photosynthetic and fermentative bacteria), are some example processes of biohydrogen production [5–7]. Once produced biologically, hydrogen can be converted to electricity using a proton exchange (PEM) fuel cell [8].

PEM fuel cells use a proton conductive polymer membrane as the electrolyte to convert hydrogen directly into electrical energy. They are particularly attractive for low (less than 1 kW) to intermediate power levels (up to 50 kW), and for applications that require rapid start-up and quick response to load changes [9,10].

It is possible to detect and estimate the amount of hydrogen produced by algae and bacteria, by transferring the gas phase accumulating over the culture medium onto a fuel cell and using equilibrium cell potential measurements and calibration curves. This leads to the possibility of a direct linkage to fuel cells to generate electrical power.

This idea of combining biologically produced hydrogen, which is an important issue in today's world in the search of renewable energy, with fuel cells for obtaining electricity has become an interesting topic for many researchers in the recent years. Some works have focused on the hydrogen production integrated to a PEM fuel cell by bacterial processes of *Rhodobacter sphaeroides* [8], *Rhodobacter capsulatus* [11], *Enterobacter asburiae* [12], anaerobic sludge [13], sludge of *Clostridium pasteurianum* and *Klepsiella* sp. [14]. Some works have focused on microalgal processes of *Chlamydomonas reinhardtii* [6,15] and *Scenedesmus obliguus* [16]. Table 1 summarizes these previous studies and approaches.

The advantage of green algae leans on the purity of the produced biogas when compared to the CO_2 mixed production by bacteria. The purity of biogas in favor of hydrogen is important for the efficiency of the PEM fuel cell because the CO_2 poisoning causes a performance loss in the proton exchange membrane fuel cells [17–19].

This work differs from others with the detailed attitude towards the fuel cell integration process. Rather than just a brief explanation it focuses mainly on the fuel cell integration and on real life experimentation. The aim of this work is to integrate a PEM fuel cell directly to a hydrogen production system incorporating *C. reinhardtii* culture. Two points constitute the novelty of this work. One is the investigation of a proper procedure for the usage of hydrogen

* Corresponding author. Tel.: +90 232 3434400; fax: +90 232 3484955.
E-mail address: suphi.oncel@ege.edu.tr (S. Oncel).

0378-7753/$ – see front matter © 2010 Elsevier B.V. All rights reserved.
doi:10.1016/j.jpowsour.2010.07.042

Nomenclature

ATP	adenosine triphosphate
PBR	photobioreactor
PEM	proton exchange membrane
PSII	photosystem-II
SPE	solid polymer electrolyte
TAP	tris–acetate–phosphate
I	current (mA)
V	fuel cell voltage (mV)
R	resistance (Ω)
P	power (mW)
P_t	theoretical power
P_{ex}	experimental power

more efficient in the fuel cell. This will be possible with the evaluation of the distinct phases in a longer batch compared to other authors [20–22] and use this data to annotate the effect on the open circuit voltage difference of the fuel cell. The other was to provide a real life application, as follow up to the work of Dante [6] who investigated the theoretical power output of an algal culture, by incorporating a commercial PEM fuel cell.

2. Experimental

2.1. Culture conditions for aerobic phase

C. reinhardtii, strain CC124, was grown photomixotrophically in 500 ml capacity bubble columns (5 cm internal diameter) in tris–acetate–phosphate (TAP) medium at pH 7.2 and about 27 °C. The cultures were continuously illuminated on one side with cool white fluorescent light (~40 μE m^{-2} s^{-1}) and sparged with sterile air–CO_2 gas mixture (3%, v/v). Algal cells in the bubble columns were grown to logarithmic phase (22 ± 2 mg Chlorophyll l^{-1}) and then inoculated (10%, v/v) into magnetically mixed (at ~450 rpm; Gerhardt MAG-H, Bonn) ROUX type flat glass photobioreactors (PBR). The total culture volume, in the ROUX type PBRs, was 1100 ml. The volume of the head space was approximately 15–20 ml. The PBRs (5.6 cm wide, 0.25 cm wall thickness) were sparged with 1 vvm gas mixture (3% CO_2) and illuminated on two sides (70 × 2 μE m^{-2} s^{-1}) by fluorescent light. The illumination system of the PBRs was modified with additional reflecting mirrors for uniformity. PBRs were directly connected to calibrated water columns to monitor the volumetric hydrogen production.

2.2. Culture conditions for hydrogen production phase

For the hydrogen production experiments aerobically cultivated cells in TAP medium, were harvested in their logarithmic phase by centrifugation (3500 × *g* for 3 min) and were then washed 5 times with sulfur depleted TAP medium (TAP-S) and resuspended in TAP-S medium to a final concentration of about 12 mg Chl l^{-1}. The hydrogen production experiments were carried out at the same temperature, mixing rate and light intensity as the aerobic phase.

2.3. Monitoring of hydrogen production and its effects on open circuit fuel cell voltage

Experiments were conducted in triplicates throughout the production at 27 °C. Two PBRs were used in parallel during each set of experiments; the first one is to measure the volumetric hydrogen production and the second one to measure the potential difference (mV) due to the produced hydrogen. For the first one, TAP-S suspended cells were put into the flat PBRs, sealed with stoppers and connected directly to calibrated water columns. For the second, the PBR was connected to a commercial PEM fuel cell (H-Tec Hydrogen Energy Systems GmbH, Germany, single plate H_2/Air PEMFC; electrode surface area 4 cm^2, with air fins on the cathode face for free interaction with the outside air) and the fuel cell was connected to the water column (Fig. 1). Water column was used for observing the gas bubbles as the indication of fuel cell is filled with gas. After the culture was transferred to the sulfur depleted medium the exhaust valve on the PEM fuel cell was closed (Fig. 1, valve 4). This dead end arrangement helped to maintain the pressure of the produced gas fed into the fuel cell.

2.4. Electricity generation

Subsequent to the start of the hydrogen production in the PBR, the feed valve and the exhaust valve of the PEM fuel cell were opened and hydrogen gas allowed to flow freely through the PEM fuel cell. When open circuit voltage reached to about 800 mV the exhaust valve was closed, returning to the dead end configuration. Later the PEM was connected to the external load. The cell voltage (mV) and cell current (mA) changes were monitored. Various external loads from 1 to 100 Ω, were tested with the same procedure.

After the load experiments, generation of electricity by the PEM fuel cells was investigated with selected loads for extended periods. The PBR was connected to the PEM fuel cell as depicted in Fig. 1. From the start of the experiment the fuel cell worked as a dead end system, in order to control the pressure and the flow of the hydrogen gas. The data for the electricity generation was recorded throughout the stable voltage value of 110 mV in all the experiments.

2.5. Analytical methods

The light intensity on the surface of the photobioreactors was measured with a quantum sensor (Licor, LI-192SA) connected to a LI-250A (Licor, Lincoln, USA) light meter.

The biogas amount, produced by the cultures, was checked using the calibrated water columns based on the water displacement amounts. Hydrogen gas formed throughout the experiment was double checked by the analysis of the samples both from the water column and from the head space of the photobioreactors. The composition of the biogas was analyzed by the injection of the biogas samples into a gas chromatograph (Agilent 6890N; Hayesep D 80/100 packed column, Argon as carrier gases) [23].

During the fuel cell experiments, in order to prevent any disturbance, samples of 1 ml volume were taken at the beginning, at the middle and at the end of the production to analyze the content of the gas by the gas chromatography.

The voltage variation on the fuel cells was monitored graphically using a flat bed data recorder (Linseis 6012, Germany). A digital multimeter (Mastech MY 64, China) was also used in order to monitor the voltage values even at low levels accurately. The electricity generated over a load resistance (1–100 Ω) was measured also with a digital multimeter connected to the fuel cell (Fig. 1). Both the recorder and the multimeter have high resolutions allowing us to detect even very small potential and current changes.

For the chlorophyll measurements, algal cells were harvested by centrifugation at 3500 × *g* for 3 min. Chlorophyll in the cells was extracted with 90% (v/v) acetone/water solution. Chlorophyll "a" and "b" amounts were determined spectrophotometrically by measuring the light absorption at different wavelengths (630, 645, 663 and 750 nm) [24]. Chlorophyll fluorescence of the cultures was determined *in situ* by a Hansatech FMS pulse modulated chlorophyll fluorimeter (Norfolk-England) by affixing the light pulse

Table 1
PEM fuel cell integration studies.

Organism	Culture medium	Operation conditions	Fuel cell	Utilization potential	Aim	Reference
Rhodobacter sphaeroides RV	Two step Pre-cultivation: aSy medium Hydrogen production: gL medium	- Anaerobic - Photosynthetic (light intensity: 107 W m^{-2}) - 30 °C - Panel type reactor (11 l, 5 cm thick) - Direct feed to PEM (88.1% H_2, 5.9% CO_2) - Batch process	PEM; Fuji Electric Corp. R&D Ltd. (800 W rated output power) Working temp.: 30 °C	10 h stable 3.7 V open circuit voltage, 1 W power	Combining photosynthetic bacterial hydrogen production with fuel cell to investigate the light energy conversion to electricity	[8]
Rhodobacter capsulatus (mutant strains)	Two step Pre-cultivation: mineral salt medium Hydrogen production: lactate, glutamate addition	- Anaerobic - Photosynthetic (light intensity: 120 W m^{-2}) - 30 °C - Stirred type reactor (3 l) - Direct feed to PEM (>90% H_2) - Batch process	PEM; H-Tec Ind. GmbH (membrane electrode assembly: 16 cm^2) Working temp.: 30 °C	22 h stable maximum values: 80 mA, 0.8 V	Comparing the potential of mutant strains for hydrogen production and their application to a fuel cell	[11]
Enterobacter asburiae SNU-1	Two step Pre-cultivation: PYG medium Hydrogen production: formic acid addition	- Anaerobic - Dark fermentation - 37 °C - Stirred type reactor (500 ml) - Direct feed to PEM - Fed batch process	PEM; specially constructed (platinum catalyst coated, Nafion 112, membrane, membrane electrode assembly: 2 cm^2) Working temp.: 25 °C	Maximum values: 0.6 Vcm^{-2}, 0.3 Acm^{-2}, 0.5 W cm^{-2}	Optimization of hydrogen production process from formic acid and its potential for the usage in fuel cell	[12]
Anaerobic sludge	Starch containing nutrient medium	- Anaerobic - Dark fermentation - 37 °C - Stirred type reactor (360 ml) - Direct feed to PEM (through KOH for CO_2 removal) - Batch process	PEM; "home made" (2 cell stack, membrane electrode assembly: 10 cm^2) Working temp.: 37 °C	1 h, maximum values: 0.428 W $cell^{-1}$, 0.65 V $cell^{-1}$	To investigate the feasibility of direct usage of hydrogen from starch containing waste water for electricity generation	[13]
Anaerobic sludge (containing: *Clostridium pasteurianum* and *Klepsiella* sp.)	Sucrose containing nutrient medium	- Anaerobic - Dark fermentation - 40 °C - Stirred type reactor, immobilize culture (3 l) - Direct feed to PEM (40.6% H_2 through NaOH for CO_2 removal; 99.9% H_2) - Continuous process	PEM; IN-540710 BCS Inc. (4 plate stack) Working temp.: 25 °C	44 h stable, maximum values: 2.28V, 0.38 A, 8.7 W	To investigate the feasibility of direct usage of hydrogen for electricity generation by dark fermentation	[14]

Table 1 (*Continued*)

Organism	Culture medium	Operation conditions	Fuel cell	Utilization potential	Aim	Reference
Chlamydomonas reinhardtii CC125	Sulfur free modified (phosphate buffer, Beijerink's medium, Hutner's solution, antibiotic)	- Anaerobic - Photomixotrophic (illumination: 40 W) - Stirred type reactor (1 l) - Direct feed to PEM - Batch process	PEM; ITESM-CCM DG01 model (1 V) Working temp.: 25 °C	48 h (volume estimation through potential of fuel cell)	Potential of fuel cell to assess hydrogen production and transient phenomena	[15]
Scenedesmus obliguus	Two step Pre-cultivation: aerated medium Hydrogen production: argon flushed and saturated sodium dithionite added anaerobic medium	- Anaerobic - Photoautotrophic (light intensity: 50 μE m^{-2} s^{-1}) - Tubular type reactor (1 l) - Direct feed to PEM - Continuous Process	PEM; H-Tec Ind. GmbH (membrane electrode assembly: 16 cm^2)	80 min stable, maximum values: 5–10 mV open circuit voltage	To investigate the easy to use bioreactor type for hydrogen production and functional coupling to a fuel cell	[16]
Chlamydomonas reinhardtii CC124	Two step Pre-cultivation: aerated TAP medium Hydrogen production: anaerobic TAP-S medium	- Anaerobic - Photomixotrophic (light intensity: 70 μE m^{-2} s^{-1}) - 27 °C - Stirred type reactor (1.1 l) - Direct feed to PEM - Batch process	PEM; H-Tec Ind. GmbH (Hydrogen/Air type fuel cell. Membrane electrode assembly: 4 cm^2) Working temp.: 27 °C	- 50 h stable 110 mV, 10 Ω load, 1.81 mA cm^{-2} - 80 h, 110 mV, 100 Ω load, 0.23 mA cm^{-2}	Investigation of the photo-biohydrogen production utilizing fuel cell. And to develop a method for the fully potential usage of fuel cell according to the biohydrogen production phases	This work

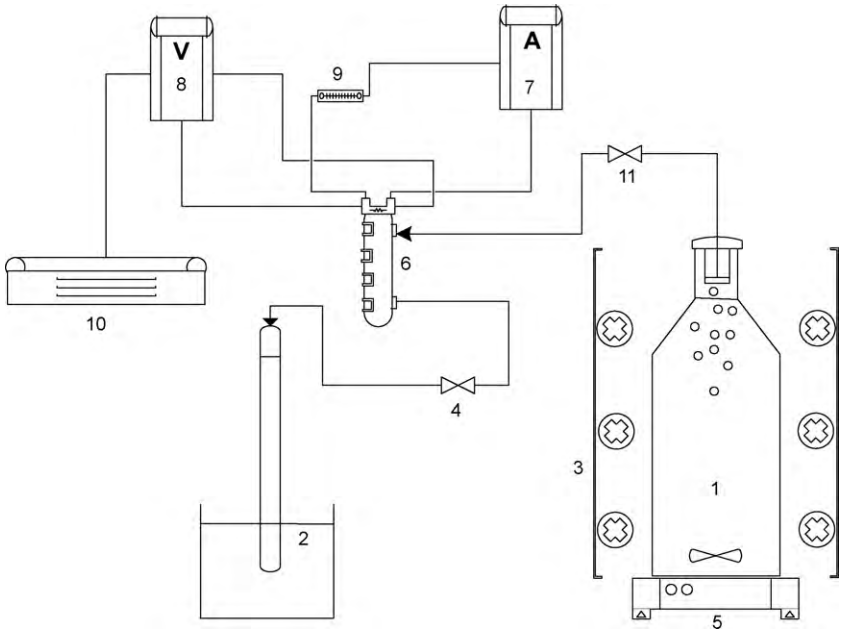

Fig. 1. Roux type PBR and feed valve (1), water column (2), light system (3), PEM fuel cell exhaust valve (4), magnetic stirrer (5), PEM fuel cell (6), digital multimeter for current (7), digital multimeter for fuel cell voltage (8), resistance load (9), flatbed recorder (10), PEM fuel cell feed valve (11).

Table 2
Culture conditions for *Chlamydomonas reinhardtii* in aerobic phase at constant light intensity ($70 \times 2\,\mu E\,m^{-2}\,s^{-1}$).

Production duration (day)	Total chlorophyll amount reached ($mg\,l^{-1}$)	Cell number ($n \times 10^6\,ml^{-1}$)	Amount of chlorophyll per cell ($mg\,Chl\,n{-}^{1}) \times 10^6$
2	24 ± 2	8 ± 1	3.1 ± 0.1

probe on the PBRs surface. Values of the three different measures were averaged for the final data.

3. Results and discussion

3.1. Growth of C. reinhardtii under photomixotrophic aerobic culture conditions

During aerobic cultivation in TAP medium the maximum cell number and chlorophyll concentration were related with the light intensity, higher intensities yielding higher values until light saturation limits. Available surface area for illumination per unit volume of the PBR also plays an important role in the efficient light usage. Better utilization of light by photosynthesis leads to a population growth which can be monitored by increase in pigments per cell during the aerobic phase of the hydrogen production. These results are also in agreement with the findings of other studies [25,26].

After the aerobic cultivation process final chlorophyll concentration of $24 \pm 2\,mg\,l^{-1}$ (cell number of $8 \pm 1 \times 10^6$ cells ml^{-1}) was the indication for the transfer into the TAP-S medium for the hydrogen production (Table 2).

3.2. Hydrogen production phase

The H_2 evolution process is induced by the sulfate nutrient deprivation of the cells, which reversibly inhibits photosystem-II (PSII) and thereby $O_2{}^-$ evolution in their chloroplasts. In the absence of sulfur, which is an essential component of cysteine and methionine, protein biosynthesis is impeded and the PSII repair cycle is blocked [27–29]. In the absence of O_2, green algae resort to anaerobic photosynthetic metabolism, in order to generate ATP, evolve H_2 in the light and consume the endogenous substrate [30,31].

The start of hydrogen production was marked with PSII activity reduction. However, maximum production was observed subsequent to obtaining gas saturation in the culture liquid, indicated by the generation of gas bubbles in the PBR. The maximum daily hydrogen production, average of triplicates, was about $44.24 \pm 3.67\,ml\,l^{-1}$ culture at day 3 (Table 3). Hydrogen production, with the Roux type PBRs, after day 3 started to decrease and dropped to lower values compared with the start, after day 7 (Fig. 2) similar to previous study [32].

There was a lag time involved for the commencement of hydrogen production. An average lag time of about 28 ± 4 h needed by the cultures for the inactivation in the photosystem 2 (Table 3). An intense loss in the PSII activities of the cultures was observed at the end of the lag time. Hydrogen production started within 2 days with a reduction at PSII about 0.275 (Table 3).

A change in the amount of chlorophyll was also observed throughout the production phase. The reduction in the amount of chlorophyll was about 40% ($12\,mg\,l^{-1}$) compared to the start of the culture (Table 3). This finding supports the results of other workers [28,33,34] and has been explained by the fact that protein biosynthesis is impeded and the PSII repair cycle is blocked through the sulfur deprivation process resulting in a destruction of chlorophyll.

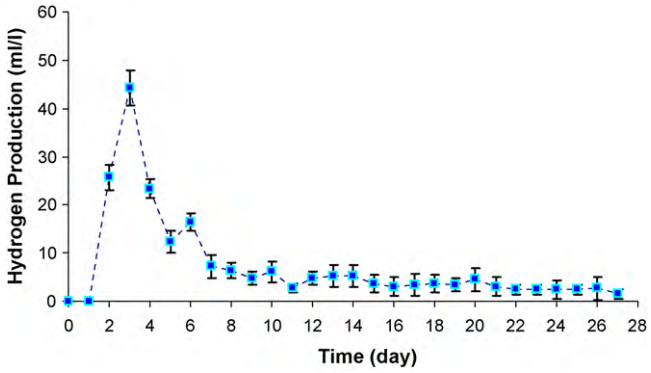

Fig. 2. Daily hydrogen production with flat PBRs ($ml\,l^{-1}\,day^{-1}$) under continuous illumination with constant light intensity ($70 \times 2\,\mu E\,m^{-2}\,s^{-1}$).

Other studies were carried out in order to investigate the potential of the PEMs directly connected to the PBRs.

3.2.1. Voltage change through the hydrogen production

When the hydrogen production graph was overlapped with the voltage change graph, it clearly shows that voltage change was almost directly proportional to the volumetric production of the hydrogen following with a delay in response (Fig. 3). This delay in the voltage response can be related to the dead end configuration. Dead end caused a pressurized environment over the head space of the PBR resulting in a need of additional time for enough gas to be produced to overcome the pressure and reach to the fuel cell to make a response [35].

Actually this delay tried to be eliminated by opening the exhaust valve. Unfortunately the free flow of the gas resulted in an unused gas escape through the fuel cell. This handicap prevented the application of this method for long term monitoring of the process (27 days).

The open circuit cell voltage changes, clearly demonstrated the various phases of the hydrogen production as defined by previous researchers [20–22] and as observed through the 35 days of batch of our previous work [32]. These phases and their relation with the voltage changes can be discussed step by step while keeping in mind that there is a delay between the volumetric productions and the responses on the voltage.

(i) *Phase 1:* This is an aerobic phase which comprises the lag phase before the production, during which photosynthetic O_2 evolution activity is gradually inactivated after the sealing of the PBR with the stopper. In this phase, no net production of hydrogen was monitored as depicted in Fig. 3 of the volumetric hydrogen change graph, thus the voltage difference continued to be negative for a while (Fig. 3: part A). This negativity may be attributed to a number of reasons. One reason might be the contamination of the anode fuel by the produced oxygen. High partial pressure of the oxygen gas in the PBR side of the fuel cell compared to the cathode side may have resulted in a negative effect similar to a reverse connected battery. Another reason could be the cell voltage decay, in other words "cell reversal" due to fuel starvation in the anode when no hydrogen gas reaches the fuel cell [36].

(ii) *Phase 2:* With the turning point A-1 when the photosynthetic O_2 evolution activity falls below the respiratory activity of the cells, leading to net O_2 consumption as depicted in the volumetric production graph, hydrogen production started. The increase in the hydrogen production is observed as the bubble formation in the PBRs (Fig. 3: part A1).

Table 3
Changes during hydrogen production phase at constant light intensity ($70 \times 2\ \mu E\ m^{-2}\ s^{-1}$).

Changes in the activity of PSII during hydrogen production phase					
At the start of the experiment	At H_2 start	% reduction in the PSII activity		At maximum H_2	% reduction in the PSII activity
0.755 ± 0.020	0.275 ± 0.020	63.58		0.065 ± 0.005	91.39
Changes during hydrogen production phase					
Lag time (h) needed for the start of the production	Start of H_2 production		Maximum H_2 production		Total H_2 in 27 days ($ml\ l^{-1}$)
	Day	Amount ($ml\ l^{-1}$)	Day	Amount ($ml\ l^{-1}$)	
28 ± 4	2	25.76 ± 2.62	3	44.24 ± 3.67	203.03 ± 24.60
Changes in total chlorophyll amount during hydrogen production phase					
Initial chlorophyll amount at the start ($mg\ l^{-1}$)		Final chlorophyll amount ($mg\ l^{-1}$)			% reduction
12		7.3 ± 0.1			39.17

Considering the voltage change, the negative effect caused by the high O_2 partial pressure in the previous phase is exceeded resulting in a slight increase in the voltage (Fig. 3: part B). But again no net change toward the positive values is observed in the voltage, because the hydrogen pressure is still not enough to reach the PEM fuel cell.

(iii) *Phase 3:* Once all O_2 in the culture medium was removed by respiration, the anaerobic phase is initiated. In this interval, hydrogen production continues to increase. This increase has a reflection on the open circuit voltage change. At point B2, the pressure of produced hydrogen is sufficient to overcome the head pressure of the PBR due to the dead end configuration, and hydrogen is transferred on to the fuel cell. At this point the voltage of the PEM fuel cell showed positive voltage (Fig. 3: part B2). During this phase although a high hydrogen production is obtained, the response of the voltage is observed with a delay, compared to the volumetric production graph of the same interval, due to the dead end configuration (Fig. 3B).

(iv) *Phase 4:* Subsequent to the establishment of complete anaerobiosis and induction of hydrogenase enzyme activity, the volume of hydrogen reaches its maximum level. In this interval hydrogen completely fills the fuel cell and an increase in the cell voltage is observed (Fig. 3: part C). Open circuit voltage raised up to 140 mV during the maximum production phase.

(v) *Phase 5:* Although the volumetric production of the hydrogen gas started to decrease open circuit voltage values maintained stable for about 100 h (Fig. 3). This persistence against decrease was due to the buffering effect of the dead end configuration because trapped hydrogen in the fuel cell continued to create a voltage difference. However as the hydrogen production continued to decrease the cell voltage started to decrease also. Eventually a sharp decrease was seen in the voltage values indicating the loss of the pressure of hydrogen in the PBR (Fig. 3: part C3). This could be attributed to the fact of fuel starvation. Results show that due to the fuel starvation, the current distribution can be uneven and a fuel cell could not present its best performance [37,38].

(vi) *Phase 6:* As the cellular activity slowed further through the end of process the voltage values of the fuel cell gradually decreased (Fig. 3: part D). The pressure loss related to the slower hydrogen production was controlled to some extent with the help of the dead end connection that enable the accumulation of the hydrogen over the head space of the PBR even during low production. This fact observed during small voltage drops followed by a stepwise increase. Examples of this stepwise formation can be seen in Fig. 3: D4. These voltage drops could be attributed to the lower mass transfer rates due to the lower hydrogen concentration on the electrolyte surface of the fuel cell [39,40].

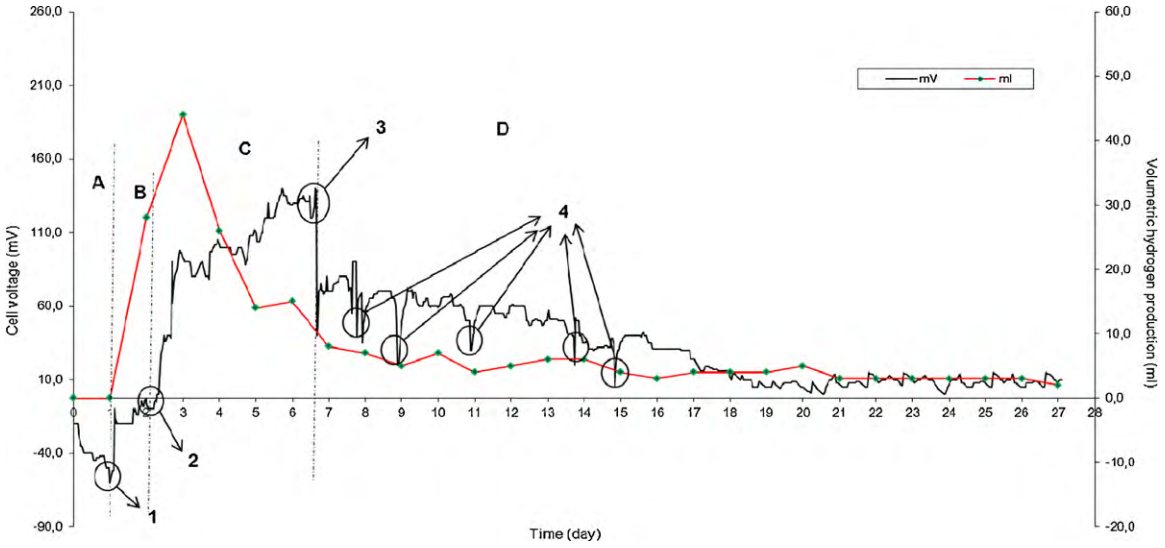

Fig. 3. Cell voltage change and average amount of volumetric hydrogen during hydrogen production phase (distinct phases of hydrogen production; A, B, C, D and sub-intervals of the phases).

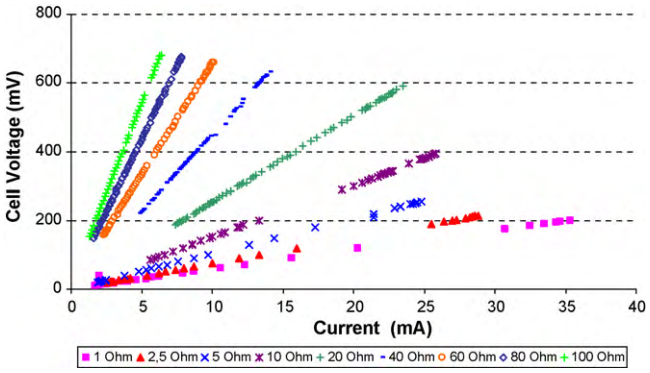

Fig. 4. Cell voltage–current generation in relation to various external load resistances.

3.2.2. *Effect of various loads on current generation of the fuel cell*

Free flow of the accumulated hydrogen through the fuel cell leads to higher voltage values, up to 900 mV (which is well suited with the characteristic limits obtained with pure hydrogen given by the manufacturer), compared to the dead end by improving the reaction rate of the fuel cell. However it also resulted in a loss of pressure and a waste of gas. Because of this fact the high values could be maintained only for few seconds. This is due to the free flow of hydrogen without any control which facilitated the easy and fast transfer of the hydrogen molecules through the membrane. This result is in agreement with the findings of other researchers [9,35].

When cell voltage was recorded against current generation (Fig. 4), it was observed that loads tested affected the current generated by the fuel cell differently. As the value of the load decreased the generated current increased, but the voltage dropped faster. This might have been considered as an expected result of Ohm's Law, however there was a contradiction which attracted attention.

When the theoretical current, calculated by Ohm's law (Eq. (1)), was compared with the experimental values, a difference was observed. This difference directly affected the power output of the fuel cell, which was the product of the cell voltage and current (Eq. (2)). When theoretical power output was compared with the experimental output to determine the efficiency (Eq. (3)), it was found that as the current generation decreased with increase in external load resistance, the efficiency increased up to 91% (Fig. 5).

$$V = I \times R \tag{1}$$

$$P = V \times I \tag{2}$$

$$\%\,\text{efficiency} = \frac{P_{ex}}{P_t} \times 100 \tag{3}$$

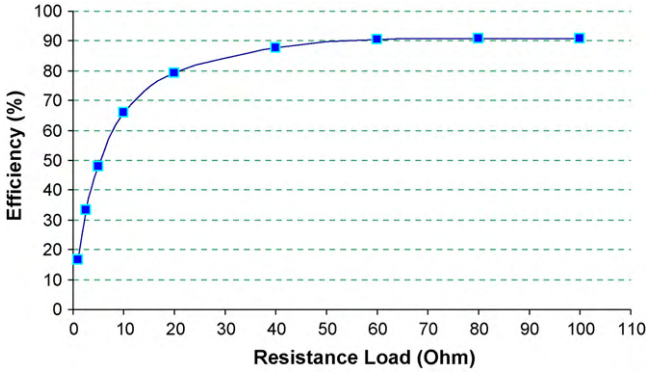

Fig. 5. Change in fuel cell efficiency with various external load resistances.

This could be attributed to a mixture of thermodynamic and kinetic factors acting in the fuel cell [41,42]. These factors effecting the efficiency were the losses due to the nature of the fuel cell defined as the start losses, resistance losses and density losses as explained by other researchers [39,40]. These losses depend on the kinetics of the electrochemical reactions (activation polarization), internal electrical and ionic resistances, and difficulties in transferring the reactants to reaction sites (mass transport limitations), internal (stray) currents and crossover of reactants in the fuel cell [10,42,43]. The nature of the PEM fuel cells used in this work could dominate the mass transfer limitations compared with the other kinetic parameters stated. The reason was, PEM constructed as a single plate and with air fins on the cathode side. The oxygen supply was possible just by the use of air through the fins which limited the extra need of oxygen during the process.

Because the feed gas has pure hydrogen, controlled by sampling through the process, the losses because of the fuel quality could be eliminated. But the production losses through the process related with the photosynthetic limitations of the culture could be a reason in the yield loss. This was also one of the main constraints of the photo-biohydrogen production, the conversion efficiencies to hydrogen could be limited [29,30]. Because of this to run even a small PEM one could need a big volume of culture.

3.2.3. *Electricity generation through online connection of PEM fuel cell*

Based on the observations from the experiments, it can be concluded that two main problems need to be solved for the better utilization for electricity generation. One is the lag time of about 2 days that is needed by the algal culture to reach to its maximum hydrogen production capacity and the second is to collect and to transfer the produced hydrogen without any loss. In order to overcome these two problems, the feed valve was closed during the lag phase for about 48 h and a dead end configuration was preferred rather than a free flow. This provided a better utilization of the produced hydrogen in the fuel cell, overcoming the response time difference between the hydrogen production and voltage change. The valve was opened after the lag phase, to reach enough pressure, and the gas was fed into the fuel cell with constant external load resistances of 10 and 100 Ω. These two loads were selected according to the efficiency values. External load of 10 Ω load lies in the rise interval of the graph and 100 Ω was at the steady state interval (Fig. 5). Thus, by selecting these two resistances, the two extreme efficiencies could be investigated. The measurement was taken at a time interval during which the voltage value was more or less stable at 110 mV for both of the tested loads. The fuel cell generated an average current of 7.22 mA for about 50 h with 10 Ω load and 0.91 mA for about 80 h with 100 Ω load. When the results of this study were compared with the theoretical values of Dante [6] who calculated that a 100 m^3 algal culture can yield an average 240 W power for 100 h, they seem to be noteworthy. On 100 m^3 base, our culture yielded a net power of 72.2 W for 50 h with a 10 Ω load and 9.1 W for 80 h with 100 Ω load, as calculated by Eq. (2), while the voltage value was kept constant at 110 mV through the process.

The difference in the values could be due to the efficiency of the fuel cell, conditions of the culture and the design of the process system including the used PEM fuel cell. In addition, the efficiency of the fuel cell with the free flow through the air fins in this study with inherent of mass transfer limitations is naturally lower than the steady flow of air or pure oxygen through the cathode side. As stated by Dante [6] the power output can vary widely depending on the use of flow rate controls. However, the results clearly demonstrate the real life potential of the system even if it is on a small scale.

4. Conclusions

The experiments carried out to study the possibility and feasibility of hydrogen production and simultaneous electricity generation with connection to PEM fuel cells resulted in a number of observations and conclusions:

(i) In open circuit the potential of the PEM fuel cell could reach up to 800 mV with an open exhaust valve in a few seconds and then decrease to lower values such as 100 mV within minutes, as observed in the load experiments.
(ii) An average of 48 h was needed to provide hydrogen with enough pressure after the start of the process.
(iii) With the dead end configuration the open circuit voltage value could only reach up to 140 mV but could maintain this level for a longer duration.
(iv) External loads caused a drastic decrease on the cell potential. As observed in the short time experiments high loads generated electricity for longer periods but with a lower power output.
(v) When the efficiency values of systems with different loads were compared, the efficiency of the 10 Ω load was found to be about 66% while the 100 Ω load yielded a 83% efficiency.
(vi) When the external load is increased 10-fold, the period of steady current generation time increased about 1.6 times. However, the power corresponding to the generated current was about 8 times higher than the one obtained with the higher external load.

The experiments conducted in this study have demonstrated that the direct usage of the PEM fuel cells showed the clear relation between volumetric change and open circuit voltage from the start to the end. To our knowledge this is the first report pointing out this potential in reference to the hydrogen production process and voltage changes. Another novelty of this work is the duration of the batch process that is monitored. This is one of the longest batches cited in literature with *C. reinhardtii* by 27 days in a ROUX type PBR. Another was a 35-day batch with a modified conventional stirred tank PBR that has a 2.5 l culture volume with online control system, again carried out by our group [32]. Furthermore, the produced hydrogen can be converted directly into energy using fuel cells, eliminating the need for a long term storage process, which is an important fact in the feasible usage of the hydrogen. These results could contribute to the development of a large scale hydrogen based electricity generation process using microalgae. However further studies need to be carried out prior to extensive utilization of this method for large scale production. Using a continuous process with direct integration of fuel cell is a plan for the future studies based on the data of the previous studies.

References

[1] R.C. Saxena, D.K. Adhikari, H.B. Goyal, Renewable and Sustainable Energy Reviews 13 (2009) 167–178.
[2] B. Johnston, M.C. Mayo, A. Khare, Technovation 25 (2005) 569–585.
[3] J.D. Holladay, J. Hu, D.L. King, Y. Wang, Catalysis Today 139 (2009) 244–260.
[4] K. Vijayaraghavan, M.A.M. Soom, Journal of Integrative Environmental Sciences 3 (2006) 55–271.
[5] S. Manish, R. Banerjee, International Journal of Hydrogen Energy 33 (2008) 279–286.
[6] R.C. Dante, International Journal of Hydrogen Energy 30 (2005) 421–424.
[7] P.C. Hallenbeck, J.R. Benemann, International Journal of Hydrogen Energy 27 (2002) 1185–1193.
[8] E. Nakada, S. Nishikata, Y. Asada, J. Miyake, International Journal of Hydrogen Energy 24 (1999) 1053–1057.
[9] F. Barbir, T. Gomez, International Journal of Hydrogen Energy 22 (1997) 1027–1037.
[10] F. Barbir, in: N. Sammes (Ed.), Fuel Cell Technology Reaching Towards Commercialization, Springer-Verlag, London, 2006, 298 p.
[11] D. He, Y. Bultel, J.P. Magnin, C. Roux, J.C. Willison, Journal of Power Sources 141 (2005) 19–23.
[12] J.H. Shin, J.H. Yoon, S.H. Lee, T.H. Park, Bioresource Technology 101 (2010) S53–S58.
[13] J. Wei, Z.T. Liu, X. Zhang, International Journal of Hydrogen Energy 35 (2010) 2949–2952.
[14] C.N. Lin, S.Y. Wu, K.S. Lee, P.J. Lin, C.Y. Lin, J.S. Chang, International Journal of Hydrogen Energy 32 (2007) 802–808.
[15] R.C. Dante, S. Armenta, M. Gutierrez, J. Celis, International Journal of Hydrogen Energy 29 (2004) 1219–1226.
[16] R. Wunschiers, P. Lindblad, International Journal of Hydrogen Energy 27 (2002) 1131–1140.
[17] G.J.M. Janssen, Journal of Power Sources 136 (2004) 45–54.
[18] F.A. de Bruijn, D.C. Papageorgopoulos, E.F. Sitters, G.J.M. Janssen, Journal of Power Sources 110 (2002) 117–124.
[19] W.M. Yan, H.S. Chu, M.X. Lu, F.B. Weng, G.B. Jung, C.Y. Lee, Journal of Power Sources 188 (2009) 141–147.
[20] A. Tsygankova, S. Kosourova, M. Seibert, M.L. Ghirardi, International Journal of Hydrogen Energy 27 (2002) 1239–1244.
[21] S. Kosourov, A. Tsygankov, M. Seibert, M.L. Ghirardi, Biotechnology and Bioengineering 78 (2009) 731–740.
[22] M.L. Ghirardi, P.W. King, M.C. Posewitz, P.C. Maness, A. Fedorov, K. Kim, J. Cohen, K. Schulten, M. Seibert, Biochemical Society Transactions 33 (2005) 70–72.
[23] N. Azbar, F.T. Dokgöz, F. Keskin, R. Eltem, K.S. Korkmaz, Y. Gezgin, Z. Akbal, S. Öncel, M.C. Dalay, C. Gönen, F. Tutuk, International Journal of Green Energy 6 (2009) 192–200.
[24] S.W. Jeffrey, N.A. Welschmeyer, in: S.W. Jeffrey, R.F.C. Mantoura, S.W. Wright (Eds.), Phytoplankton Pigments in Oceanography: Guidelines to Modern Methods, UNESCO Publishing, 1997, 661 p.
[25] J.C. Ogbonna, H. Yada, H. Tanaka, Journal of Fermentation and Bioengineering 2 (1995) 369–376.
[26] J.C. Ogbonna, H. Yada, H. Masui, H. Tanaka, Journal of Fermentation and Bioengineering 82 (1996) 61–67.
[27] M.L. Ghirardi, L. Zhang, J.W. Lee, T. Flynn, M. Seibert, E. Greenbaum, A. Melis, TIBTECH 18 (2000) 506–511.
[28] A. Melis, L. Zhang, M. Forestier, M.L. Ghirardi, M. Seibert, Plant Physiology 122 (2000) 127–135.
[29] L. Zhang, T. Happe, A. Melis, Planta 214 (2002) 552–561.
[30] A. Melis, Planta 226 (2007) 1075–1086.
[31] S. Kosourov, V. Makarova, A.S. Fedorov, A. Tsygankov, M. Seibert, M.L. Ghirardi, Photosynthesis Research 85 (2005) 295–305.
[32] S. Oncel, F. Vardar-Sukan, International Journal of Hydrogen Energy 34 (2009) 7592–7602.
[33] J.P. Kima, C.D. Kang, T.H. Park, M.S. Kim, S.J. Sim, International Journal of Hydrogen Energy 31 (2006) 1585–1590.
[34] A. Melis, Trends in Plant Science 4 (1999) 130–135.
[35] C.W. Woo, J.B. Benziger, Chemical Engineering Science 62 (2007) 957–968.
[36] F.A. Bruijn, V.A.T. Dam, G.J.M. Janssen, Fuel Cells 1 (2008) 3–22.
[37] D. Liang, Q. Shen, M. Hou, Z. Shao, B. Yi, Journal of Power Sources 194 (2009) 847–853.
[38] Z. Liu, L. Yang, Z. Mao, W. Zhuge, Y. Zhang, L. Wang, Journal of Power Sources 157 (2006) 166–176.
[39] S.R. Huang, C.Y. Lin, C.C. Wu, S.T. Liu, L.C. Lin, S.J. Yun, International Journal of Hydrogen Energy 33 (2008) 1598–1606.
[40] M.W. Fowler, R.F. Mann, J.C. Amphlett, B.A. Peppley, P.R. Roberge, Journal of Power Sources 106 (2002) 274–283.
[41] R.C. Dante, J.L. Escamilla, V. Madrigal, T. Theuss, J.D. Calderon, O. Solorza, R. Rivera, International Journal of Hydrogen Energy 28 (2003) 343–348.
[42] F. Barbir, H. Gorgun, X. Wang, Journal of Power Sources 141 (2005) 96–101.
[43] M.V. Moreira, G.E. Silva, Renewable Energy 34 (2009) 1734–1741.